Available online at www.scholarsresearchlibrary.com

Scholars Research Library

Archives of Physics Research, 2014, 5 (1):1-11
(http://scholarsresearchlibrary.com/archive.html)

Scholars Research Library
ISSN : 0976-0970
CODEN (USA): APRRC7

Study of Er^{3+} and Er^{3+}/Yb^{3+} Co-doped tellurite glass for communication

Ibrahim D. A.[a], S. K. Singh[a] and S. B. Rai[b]

[a]*Department of Pure and Applied Physics, Adamawa State University, Mubi, Nigeria*
[b]*Laser and Spectroscopy Laboratory, Department of Physics, Banaras Hindu University, Varanasi, India*

ABSTRACT

Erbium and Erbium/Ytterbium co-doped tellurite glasses have been prepared by melt quench technique. Two characteristic band; at 650 – 660 cm^{-1} (axial band) and at 725 -785 cm^{-1} (equatorial band) of TeO_2 are exhibited in the spectrum. Up conversion emission spectra of Er^{3+}/ Yb^{3+} co-doped sample under 976nm excitation is studied., which revealed four prominent emission bands at 531, 548, 670 and 846 nm originating from $^2H_{11/2} \rightarrow {}^4I_{15/2}$, $^4S_{3/2} \rightarrow {}^4I_{15/2}$, $^4F_{9/2} \rightarrow {}^4I_{15/2}$ and $^4S_{3/2} \rightarrow {}^4I1_{13/2}$ transitions, respectively, which is most intense in green region. Down conversion of singly doped Er^{3+} tellurite glasses under 532nm excitation is also studied which showed emission bands centered at 548, 660, 797, 847 and 976 nm attributed to $^2H_{11/2} + {}^4S_{3/2} \rightarrow {}^4I_{15/2}$, $^4F_{9/2} \rightarrow {}^4I_{15/2}$, $^2H_{3/2} \rightarrow {}^4I_{13/2}$, $^4S_{3/2} \rightarrow {}^4I_{13/2}$ and $^4I_{11/2} \rightarrow {}^4I_{15/2}$ transitions, respectively. The variation of luminescence intensity at different laser excitation powers is observed. Near infrared radiation has been generated.

INTRODUCTION

Luminescent materials have been a subject of intense study for more than three decades due to their potentiality for various applications. The search for novel materials with better luminescent properties has intensified in recent years as many novel applications have emerged. A major class of fluorescent metal ions is the Rare Earths family which has been the most explored for applications ranging from laser physics to molecular biology [1-4]. The rare-earths have high luminescence efficiencies in the visible region [5-7]. Glasses doped with rare-earth ions are important laser materials and have many other applications e.g. in eye-safe goggles, as protection against high energy neutrons etc

[8-10]. Despite their relative scarcity in the earth's crust (as the name itself signifies) the nature of their electronic energy levels involving the $4f^n$ configuration is one of the main reasons for their extensive use. The Nd: glass lasers and Er-doped polymer amplifiers are just two well known examples of the versatility of rare earths as luminescent materials.

Most of the solid state lasers available at the moment involve a trace amount of ionized rare earth or transition metal ion doped in a crystal or glass lattice. Many glass and crystal systems have been investigated in order to develop an understanding of the influence of the host materials on the laser properties of the active material. Most of the earlier lasers utilized crystals such as yttrium, aluminum garnet, ruby, CaF_2 etc as host materials [11]. However in recent years glasses are being increasingly used as laser host. In fact glasses have several advantages over crystals as laser host. Glass can be produced in large volumes with high optical homogeneity. The nonlinear refractive indices can be made low enough [12] and the concentration of active materials in the glass host can be made much larger than in

crystals.These examples clearly demonstrate that the study of doped glasses is an important and productive field in modern optics and optoelectronics and needs continued attention.

In the past decades, the Er^{3+} ions doped materials have effectively been studied for lasers and optical amplifiers. Most recently, their upconversion luminescence exhibits extensive applications in color display, fluorescent labeling, white light simulation, biomedical diagnostics, optical temperature sensors etc. ([13-16]. It is one of the most commonly used rare earth ion that provides up-converted visible fluorescence both in fluoride [17] and oxide glasses matrices [18]. It is one of the efficient active centers and has a favorable energy level structure with two transitions: $^4I_{15/2} \rightarrow {}^4I_{11/2}$ (at about 980 nm) and $^4I_{15/2} \rightarrow {}^4I_{9/2}$ (at about 800 nm) which can be efficiently excited with high power semiconductor lasers, yielding blue, green, and red emission bands. For the upconversion emissions in many Er^{3+} doped or Er^{3+}/Yb^{3+} co-doped materials, when pumped at 980 nm, the luminescence found is in green and red regions [19-22].

MATERIALS AND METHODS

Four glass samples with the following analytical compositions were prepared.
(a) 79.5%TeO_2 + 20%$BaCO_3$ + 0.5%Er_2O_3
(b) 79%TeO_2 + 20%$BaCO_3$ + 1%Er_2O_3
(c) 78.5%TeO_2 + 20%$BaCO_3$ + 1.5%Er_2O_3
(d) 76%TeO_2 + 20%$BaCO_3$ + 1%Er_2O_3 + 3%Yb_2O_3

The melt-quench sampling technique has been used for the glass samples preparation. Appropriate weight ratios of starting materials given above were taken in their pure form. The required powder materials were thoroughly crushed and well mixed in an agate mortar homogeneously. Each homogeneous mixture was transferred to a platinum crucible (melting point of about 1773^0C) and heated in an electric oven to melt at 900^0C for about 30 minutes. The melt was then poured into a preheated brass mould and annealed at 200^0C for about two hours to remove thermal strains. This was then cooled to room temperature gradually. The samples were then cut into proper shapes and sizes and polished carefully for optical measurements. These samples were immediately stored in a vacuum desiccator to prevent possible attach by moisture and contamination until used for measurement.

In order to record the absorption spectra the samples in UV-VIS/NIR regions, a Cary 2390 (Varian Associates) double beam UV-VIS/NIR spectrophotometer was used. During these measurements the incident light from the source is divided into two beams and allowed to fall on an optical chopper. The optical chopper is so arranged that while its half part is open, the other half is covered with reflecting mirrors. Thus for one half of the cycle, one beam is reflected. The transmitted beam passes through the rare earth doped glass sample kept in its path with the help of a sample holder. After passing through the glass sample the transmitted beam travels in almost identical distance (through an undoped identical glass piece) and finally goes to another photo-detector. This compensates for any absorption by the atmosphere. The difference of the two signals is fed to the recorder to obtain the final spectrum. The absorption spectrum is shown in Fig 2. For fluorescence spectrum, we used monochromator detector system, Ocean Optics QE65000 TE cooled CCD spectrometer . Nd:YAG laser (CW, 532nm wavelength) and Diode laser (CW, 976nm wavelength with 1 watt) were used as excitation sources. Initially, a beam from a laser source like 976 nm diode laser or 532 nm Nd-YAG laser falls on a front coated mirror (Fig. 1). Then after reflecting at an angle 90^0 the beam falls on a convex lens which converges the beam on to the sample placed at its focal point. The glass sample starts emitting after absorbing the radiation. The radiated emission is collected and recorded by a CCD spectrophotometer placed at an angle 90^0 to the beam incident on the sample. The CCD spectrophotometer is connected to the computer via a data cable. Thus emission radiated by the sample is directly seen on the screen of monitor through a wavelength vs emission intensity plot and its data is automatically saved on the computer. Repeated measurements were carried out to get good signal and also to see the effect of laser power.

The FTIR spectra of the samples were recorded using Perkin Elmer Spectrum RX1 spectrophotometer. The glass samples were powdered and a pellet was prepared in KBr to record the spectrum in the 4000-400 cm^{-1} spectral region with $4cm^{-1}$ resolution, auto gain and 40 scans.

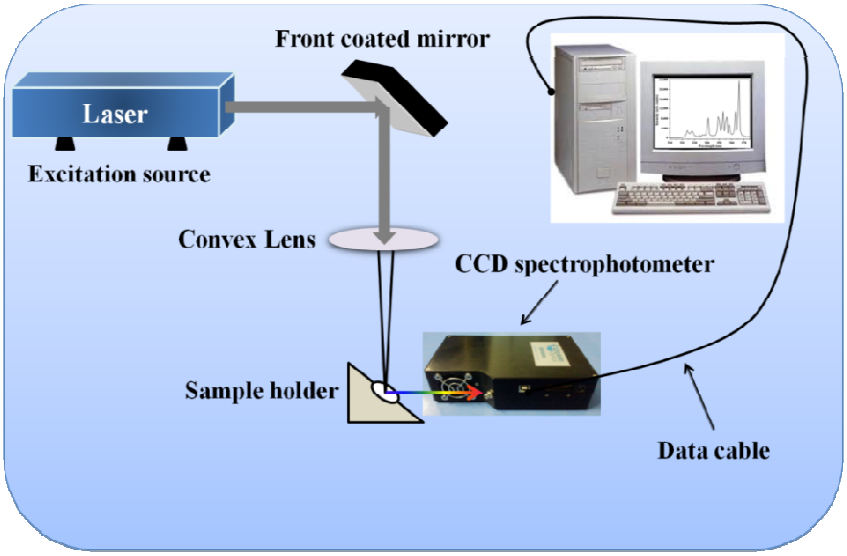

Figure 1 Experimental setup for luminescence and upconversion measurements

RESULTS AND DISCUSSION

3.1. Absorption Spectrum

Fig. 1 illustrates the absorption spectra of the Er^{3+} and Er^{3+}/Yb^{3+} co-doped tellurite glasses in the visible and near-infrared region from 360- 1200 nm. The absorption spectrum consists of seven absorption bands of Er^{3+} peaked at 450, 489, 522, 545, 653, 800, and 980 nm corresponding to the absorptions from the ground state $^4I_{15/2}$ to the excited states $^4F_{5/2}$, $^4F_{7/2}$, $^2H_{11/2}$, $^4S_{3/2}$, $^4F_{9/2}$, $^4I_{9/2}$, and $^4I_{11/2}$ respectively. In addition, the strong absorption band peaked at 976 nm correspond to the ground state absorption of Yb^{3+}. It is noted that, the excited state $^2F_{5/2}$ of Yb^{3+} is in the same region in which the $^4I_{11/2}$ level of Er^{3+} lies. Since Yb^{3+} has a much broader absorption band from 860 to 1085 nm, and the absorption crosssection of Yb^{3+} is many times larger than that of the Er^{3+}. Hence, the addition of Yb^{3+} enhances the pumping efficiency of 976 nm diode laser through the energy transfer from Yb^{3+} to Er^{3+}. The energy transfer takes place through the mechanism: $^2F_{5/2}(Yb^{3+})^* + {}^4I_{15/2}(Er^{3+}) \rightarrow {}^2F_{7/2}(Yb^{3+}) + {}^4I_{11/2}(Er^{3+})^*$. So the energy transfer process acts as indirect pumping of Er^{3+}. Due to the strong absorption of glass hosts in the ultraviolet region, the absorption bands at the wavelength shorter than 400 nm could not be distinguished. In addition, the cutoff bands are lower than 400 nm, indicating that the energy transfer (ET) from Er^{3+} to the band gap of glass matrix can be neglected [23].

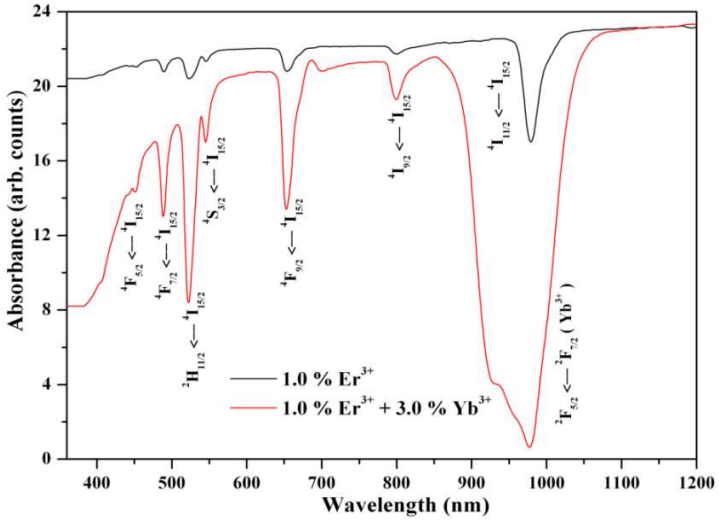

Figure 2. Absorption spectra of Er^{3+} and Er^{3+}/Yb^{3+} co-doped tellurite glasses(sample b and d) from visible to near infrared region

3.2 Fourier Transform Infrared (FTIR) measurements

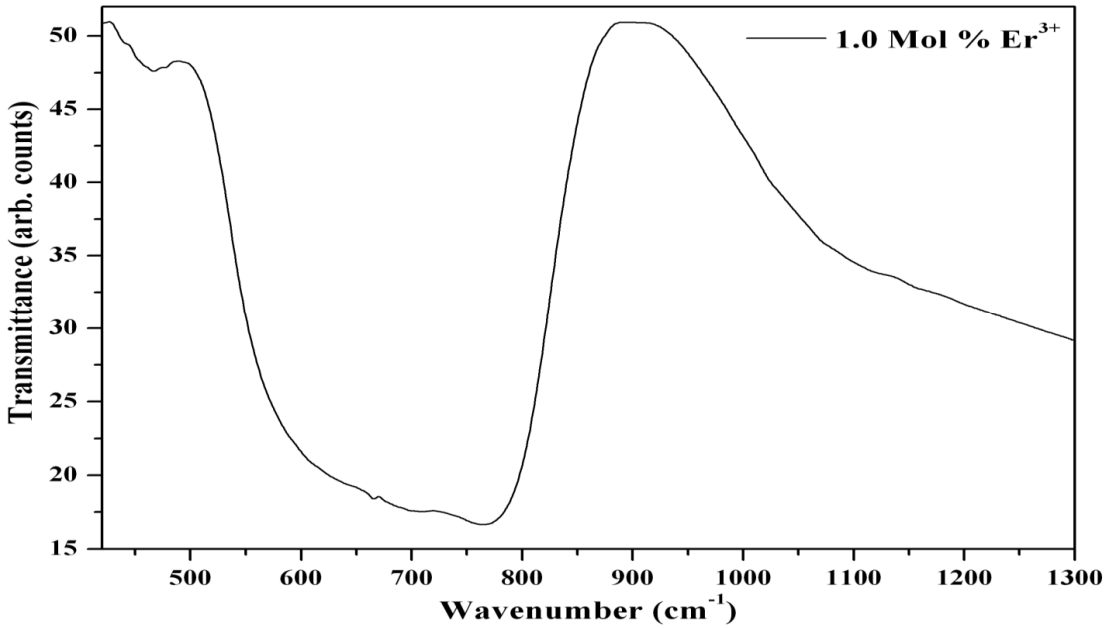

Figure 3 FTIR spectrum of 1.0 Mol% Er^{3+} doped barium tellurite glass

As shown in Fig. 3, the FTIR spectrum shows that the TeO_2 is the glass former while $BaCO_3$ is the glass modifier in the barium tellurite glass system. The role of barium ions as network modifier is to modify the glass structure and enhance the breaking of axial Te-O-Te linkages in the trigonal bipyramids [TeO_4] (tbp) and create the formation of trigonal pyramid [TeO_3] (tp) units and non-bridging oxygen. A diffuse band is observed in the range of 500-600 cm^{-1}, due to the disordered structure; this is considered as the vibration modes of both the TeO_3 and the TeO_4 entities [24]. The vibration modes of the bonds for TeO^{3+1} polyhedral are also found at bands around 580 cm^{-1}. The spectrum has exhibited two characteristic bands at 650-660 cm^{-1} (axial band) [25-26] and at 725-785 cm^{-1} (equatorial band) [27-28] of TeO_2.

3.3 Upconversion luminescence spectra

The upconversion emission spectra (500-880 nm) of Er^{3+}/Yb^{3+} co-doped tellurite glass has been recorded using 976 nm diode laser excitation at room temperature and shown in Fig. 4a and 4b. Mainly four intense upconversion emission bands centered at 531, 548, 670 and 846 nm have been observed which are attributed to $^2H_{11/2} \rightarrow {}^4I_{15/2}$, $^4S_{3/2} \rightarrow {}^4I_{15/2}$, $^4F_{9/2} \rightarrow {}^4I_{15/2}$ and $^4S_{3/2} \rightarrow {}^4I1_{3/2}$ transitions, respectively. These transitions are associated with Er^{3+} ions. It is apparent that the green emission at 548 nm has the highest peak intensity. The intensity of red emission at 670 nm is much weaker than that of green emission at 546 nm. Fig. 4.4b shows the efficient energy transfer from Yb^{3+} to Er^{3+} ions. The Er^{3+} doped glass shows a very weak green emission. Addition of Yb^{3+} enhances the overall emission several times. It should be noted that the upconversion emission in Er^{3+}/Yb^{3+} doped tellurite glass is so efficient that the green emission can be seen by naked eyes with pump power as low as a 20 mW. Fig. 4a shows the emission of tellurite glass doped with 1.0Mol % of Er^{3+} and 3.0Mol % of Yb^{3+} ions with increasing incident laser power. It can be seen easily that the overall emission increases very rapidly with pump power. The dependence of emission intensity on incident power could also be recorded at different power. This permitted us to determine the number of photons involved in the process.

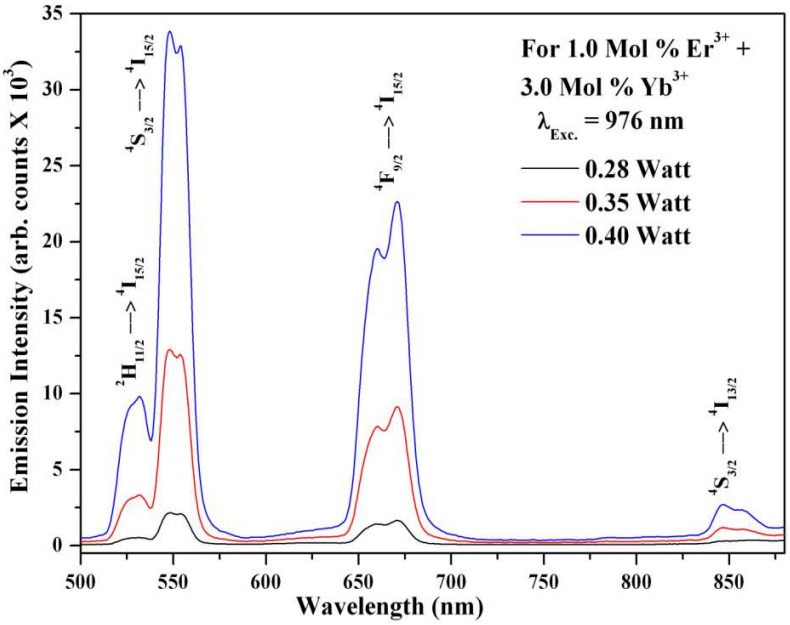

Figure 4a Emission spectra of sample (d) excited with 976nm Diode laser

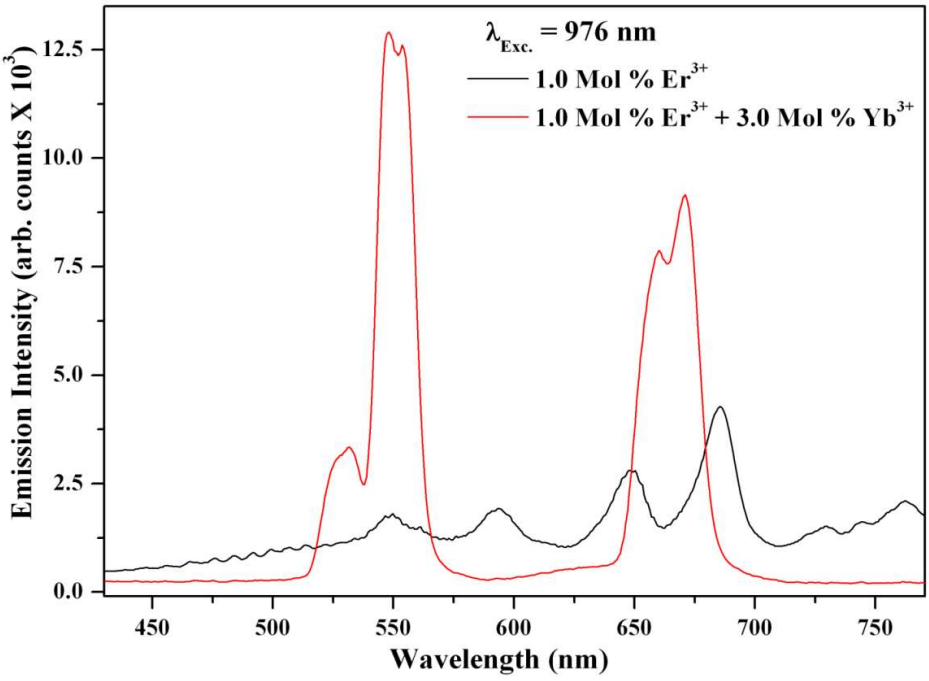

Figure 4b A comparison of emission spectra of Er^{3+} in the presence and absence of Yb^{3+}

3.4 Downconversion luminescence spectra

Fig. 4(c-i) show the downconversion luminescence spectra of Er^{3+} and Er^{3+}/Yb^{3+} doped tellurite glass samples with 532 nm Nd-YAG laser at different concentration of Er^{3+} ions and at different incident laser powers. The downconversion emission spectra were recorded in the wavelength 540-1035 nm. Five downconversion emission bands centered at 548, 660, 797, 847 and 976 nm have been observed which are attributed to $^2H_{11/2} + {}^4S_{3/2} \rightarrow {}^4I_{15/2}$, $^4F_{9/2} \rightarrow {}^4I_{15/2}$, $^2H_{3/2} \rightarrow {}^4I_{13/2}$, $^4S_{3/2} \rightarrow {}^4I_{13/2}$ and $^4I_{11/2} \rightarrow {}^4I_{15/2}$ transitions, respectively. Fig. 4.4c shows the emission of

tellurite glass doped with 1.0Mol % of Er^{3+} and 3.0Mol % of Yb^{3+} ions with increasing incident laser power. It is observed that the overall emission i.e. of green, red and near infrared region increases with laser power.

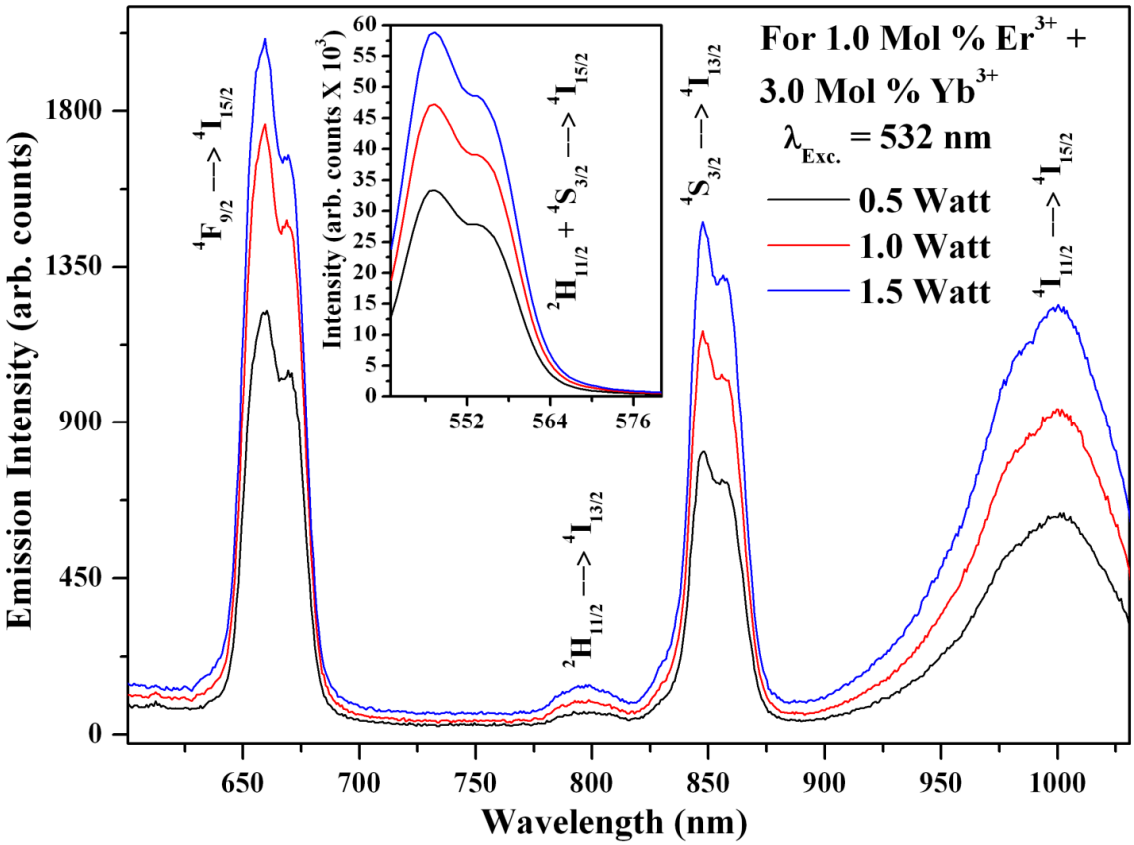

Figure 4c Emission spectra of sample (d) excited with 532nm Nd-YAG laser

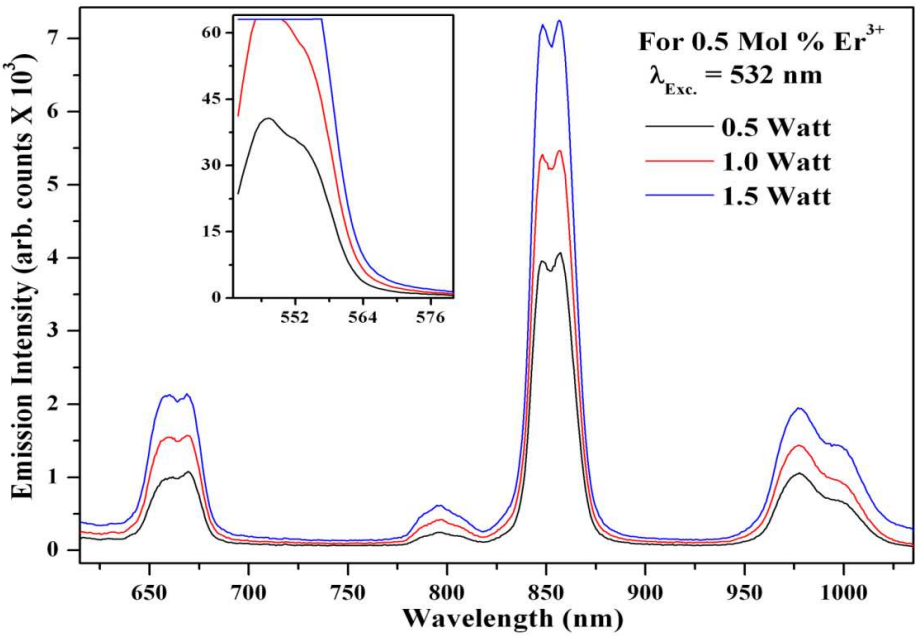

Figure 4d Emission spectra of sample (a) excited with 532nm Nd-YAG laser

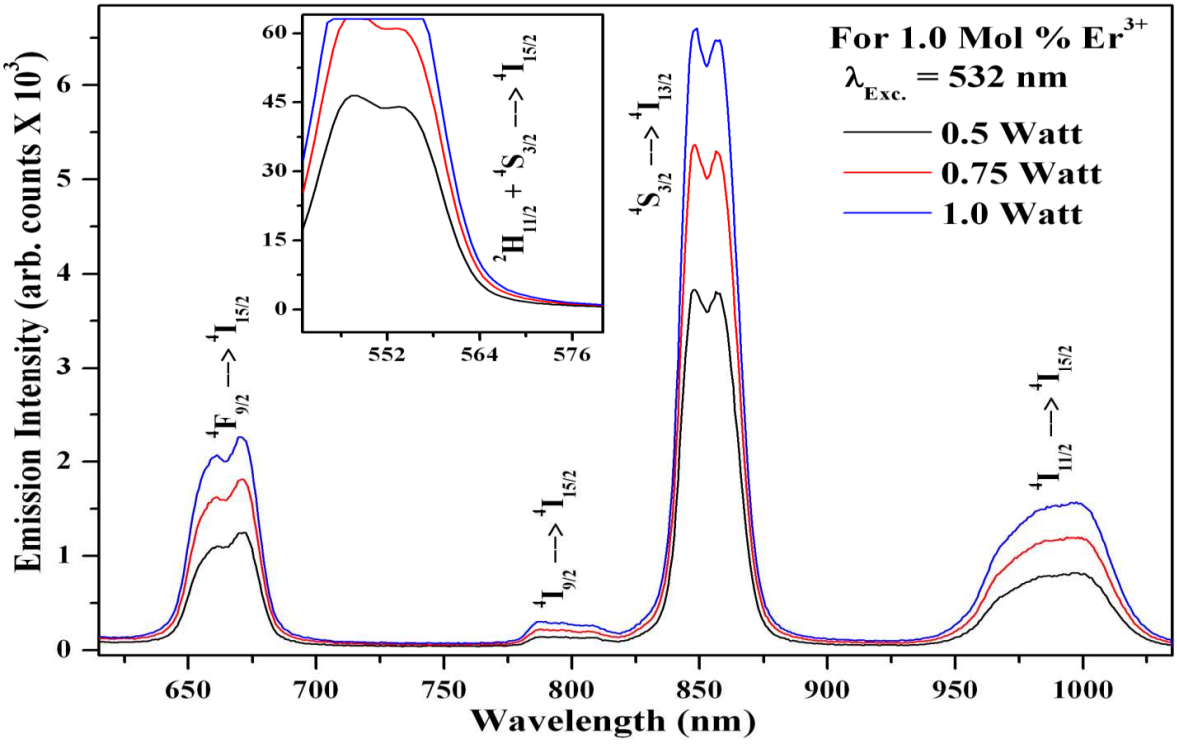

Figure 4e Emission spectra of sample (b) excited with 532nm Nd-YAG laser

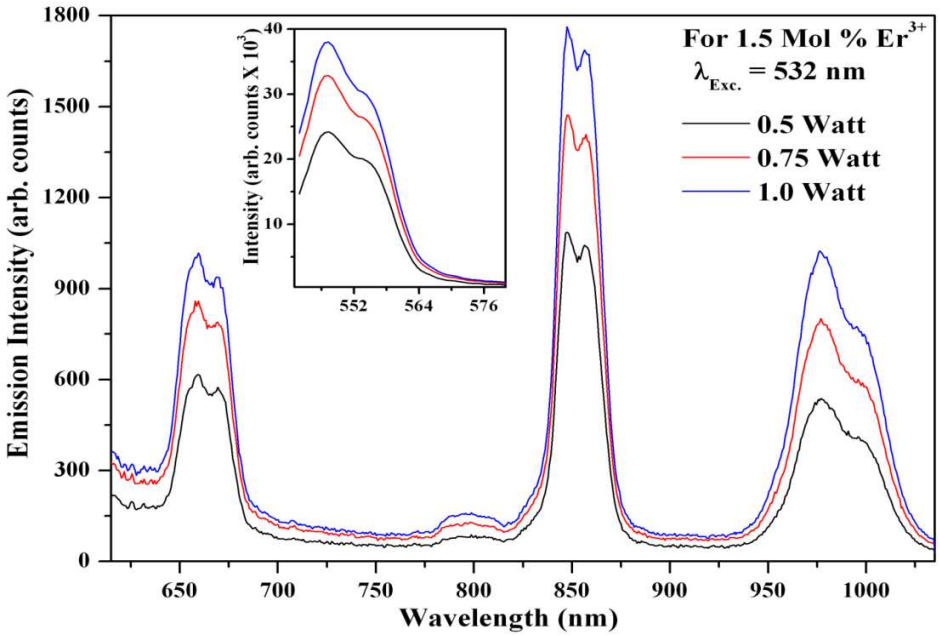

Figure 4f Emission spectra of sample (c) excited with 532nm Nd-YAG laser

In fig. 4(d-f) the concentrations of Er^{3+} ions was fixed for three values i.e. 0.5, 1.0 and 1.5 Mol % and the effects of incident laser power for three values i.e. 0.5, 1.0 and 1.5 Watt on emission of Er3+ ions were observed. It is seen that the emission intensity increases with laser power in all the three cases. The inset in these figures shows the emission of green region from 541-580 nm.

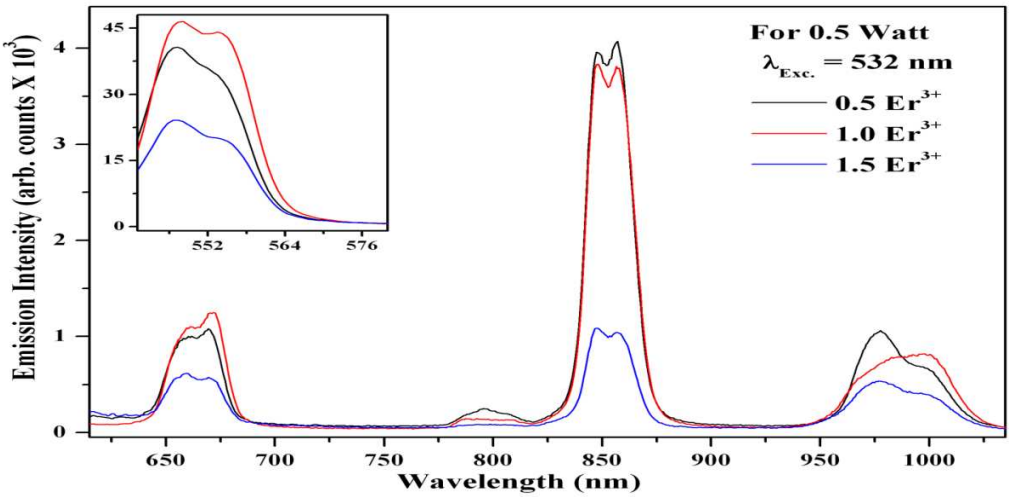

Figure 4g A comparison of emission spectra of samples (a), (b) and (c) for 0.50W Nd-YAG laser power

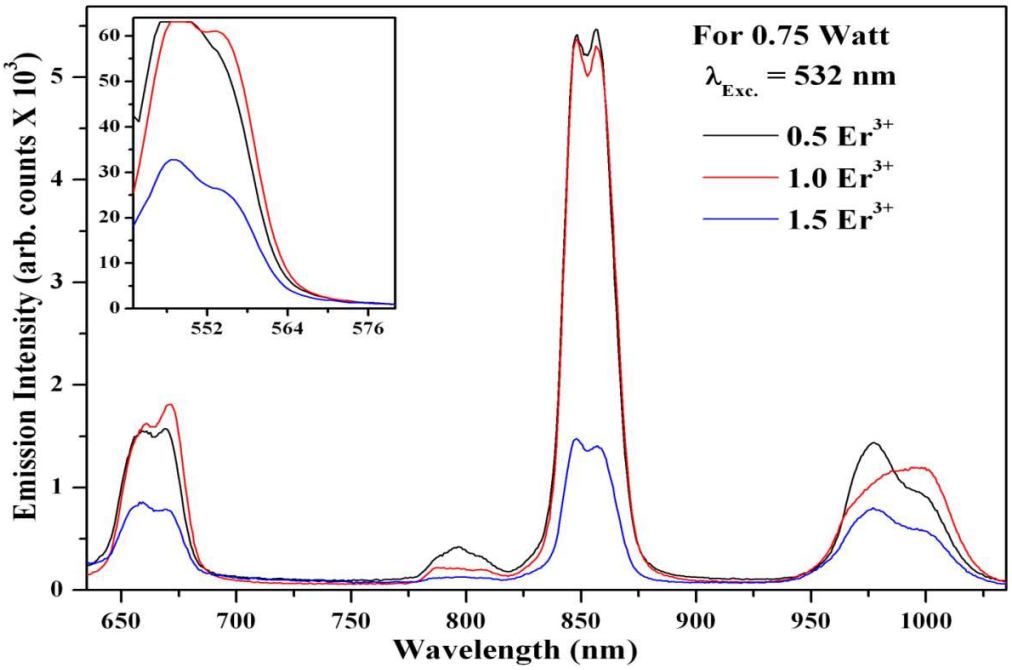

Figure 4h A comparison of emission spectra of samples (a), (b) and (c) for 0.75W Nd-YAG laser power

In fig. 4(g-i), the incident laser power was kept the same for three concentrations of Er^{3+} i.e. 0.5, 1.0 and 1.5 Mol% and the emission of Er^{3+} ions was recorded for three values of pump power viz 0.5, 0.75 and 1.0 watt power. In this case, it is found that on increasing the concentration of Er^{3+} ions in the sample, the emission intensity of red band initially increases slightly and then reduces slowly. But the emission of near infrared region i.e. 797, 847 and 976 nm decreases continuously with increasing Er^{3+} concentration initially slightly and then sharply. The inset in these figures shows the emission of green region from 541-580 nm.

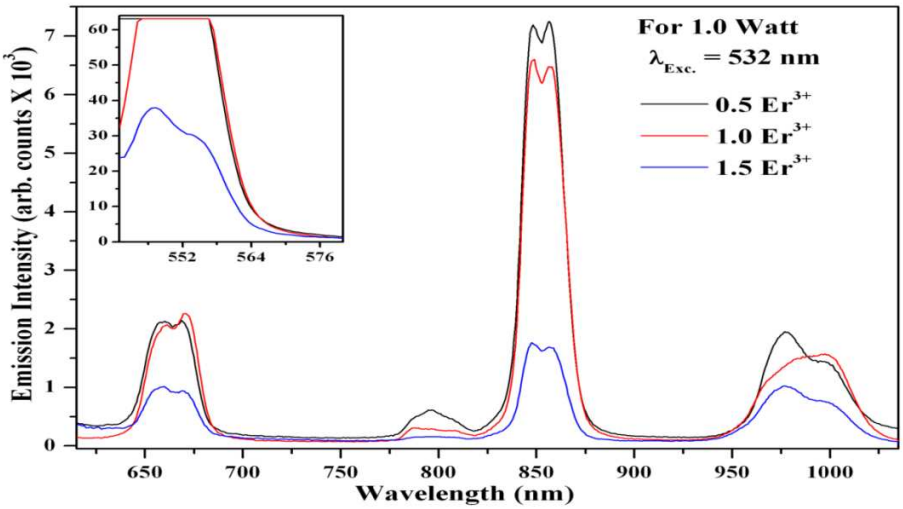

Figure 4i A comparison of emission spectra samples (a), (b) and (c) for 1.00W Nd-YAG laser power

3.5 Mechanism of upconversion emission (Energy level diagram)

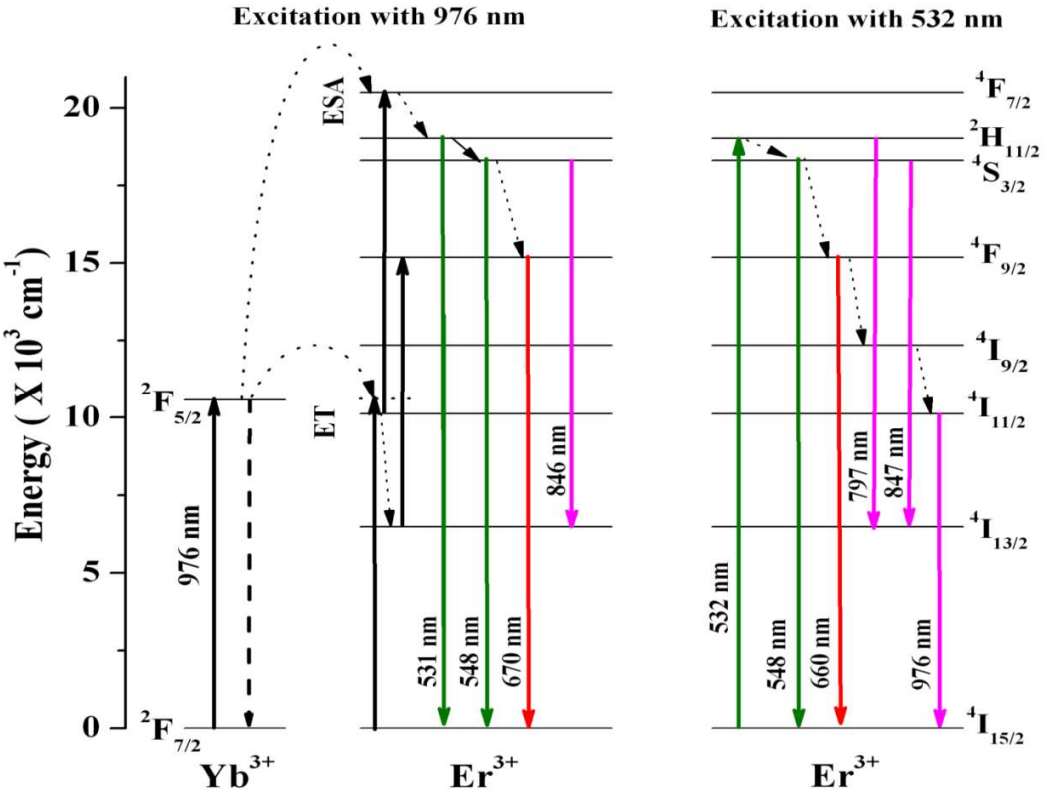

Figure 4.5 Schematic energy level diagram of Er^{3+} Yb^{3+} ions showing possible upconversion emission mechanisms

According to the energy matching conditions, the possible upconversion mechanisms for the green, red and near infrared emissions are discussed based on the energy level diagram of Er^{3+} and Yb^{3+} presented in fig. 4.5. Initially Yb^{3+} ions in the $^2F_{7/2}$ state (ground state) absorb 976 nm photons from diode laser and excite them to the $^2F_{5/2}$ state. The second step involves the excitation of Er^{3+} ions in the $^4I_{11/2}$ level by means of the energy transfer process from excited Yb^{3+} to Er^{3+} : $^2F_{5/2}$ (Yb^{3+}) + $^4I_{15/2}$ (Er^{3+}) → $^2F_{7/2}(Yb^{3+})$ +$^4I_{11/2}$ $(Er^{3+})^*$. Er^{3+} ions in $^4I_{11/2}$ level again absorb

pumping photon 976 nm radiation and excite Er^{3+} from $^4I_{11/2}$ to the $^4F_{7/2}$ level of Er^{3+}. The populated $^4F_{7/2}$ level then relaxes rapidly (nonradiatively) to the next lower lying excited levels $^2H_{11/2}$ and $^4S_{3/2}$. The population of the $^4S_{3/2}$ level can also be affected by a fast multiphonon decay from the $^2H_{11/2}$. The above processes then produces the three transitions $^2H_{11/2} \rightarrow {}^4I_{15/2}$, $^4S_{3/2} \rightarrow {}^4I_{15/2}$ and $^4S_{3/2} \rightarrow {}^4I_{13/2}$ in green region centred at 531 nm and 548 nm and in NIR region centred at 846 nm, respectively. A part of population of Er^{3+} ions relaxes nonradiatively to the next lower lying excited levels $^4F_{9/2}$ and $^4I_{9/2}$. Besides, Er^{3+} in the $^4I_{11/2}$ state relaxes nonradiatively to $^4I_{13/2}$ level. Er^{3+} ions in this level again absorb incident photon from laser and reach to $^4F_{9/2}$ level. The red emission centred at 670 nm is originated from the $^4F_{9/2} \rightarrow {}^4I_{15/2}$ transition. The mechanism is based on the processes as follows: $^4I_{13/2}$ (Er^{3+}) + hν → $^4F_{9/2}$ (Er^{3+}) and $^4F_{9/2} \rightarrow {}^4I_{15/2}$ + hν(670nm). All up-conversion luminescence discussed above are nonlinear two-photon process [29-30].

In case of 532 nm excitation Er^{3+} ions reach to their highly excited state $^2H_{11/2}$ after absorbing 532 nm laser radiation in the ground state $^4I_{15/2}$. From this state Er^{3+} ions relax to different lower lying excited states i.e. $^4S_{3/2}$, $^4F_{9/2}$, $^4I_{9/2}$, and $^4I_{11/2}$ nonradiatively. Finally ions come to ground state from these excited states by emitting green, red and near infrared transitions.

CONCLUSION

The $(80-x)TeO_2$ + $20BaCO_3$ + xEr_2O_3 (where x = 0.5, 1, 1.5 Mol%) and $76\%TeO_2$ + $20\%BaCO_3$ + $1\%Er_2O_3$ + $3\%Yb_2O_3$ glass systems have been prepared using melt quench technique. The FTIR spectra showed that the addition of $BaCO_3$ enhanced the breaking of the axial Te-O-Te linkages in the trigonal bipyramids [TeO_4] and formed the trigonal pyramids with non-bridging oxygen during the formation of the glass. The vibrational modes of the bonds for TeO^{3+1} polyhedral were found around $580cm^{-1}$.

Co-doping Er^{3+} with Yb^{3+} enhanced the pumping efficiency of the 976nm diode laser through the energy transfer from Yb^{3+} to Er^{3+}. Subsequently, an intense upconversion emission (a two photon process) in the green region was clearly seen by naked eye even with a low pump power as 20mW. The overall upconversion increases with increasing the laser power. Again, the downconversion observed in the samples doped with only Er^{3+} also showed that emission intensity increases with increasing laser power. The intensity is most intense in the near infrared region (NIR) and best for sample (a) with lowest concentration of Er^{3+}. NIR emissions were observed in the downconversion properties of 0.5Mol% Er^{3+} doped tellurite glass which originates from $^4S_{3/2} \rightarrow {}^4I_{13/2}$ transition. This may be applicable in fiber optic fabrication for use in optical communication. The fluorescence intensity is enhanced on addition of Yb^{3+}.

Acknowledgements
Financial support in the form of Fellowship from Adamawa State University/Education Trust Fund/TET Fund is gratefully acknowledged.

REFERENCES

[1] Steckel, A. J. and Zavada, J. M., (**1999**),
MRS bulletine, **24**, 33-38.
[2] Kenyon, A. J., (**2002**), *Progress in quantum electronics*, **26**, 225-284.
[3] Kik, P. G. and Ploman, A., (**1992**), *MRS bulletin*, **23**, 48-54.
[4]Chiasera, A., Tosello, C., Moser, E., Montanaga, M., Belli, R., Goncalves, R. R., Righini, G. C., Pelli, S., Chiappini, A., Zampedri, L. and Ferrari, M., (**2003**), *Journal of Non crystalline solids*, **322**, 289-294.
[5] Sherman, J. L., (**2006**), New research on optical materials, Nova Science Publishers,
[6]Wegh, R. T., Donkjer, H., Oskam, K. D. and Mijerink, A., (**1999**), *J. Non-Cryst. Solids*, **283**, 663-666.
[7] Yen, W. M., Shionoya, S. and Yamamoto, H., (**2006**), Practical application of Phosphors CRS Press, Taylor and Francis Group, FL.
[8] Lucas, J., (**1995**), *J. Flourine Chem.*, **72**, 177-181
[9]Bellemans, F., De Corte, F. and Van Den Haute, P., (**1995**), *Radiation Measurements*, **24**, 153-160.
[10] De Souza, J. M., Nunes, L. A. O., Rohling, J. H. and Baeses, M. L., (**2003**), Laser Emission at 1077 nm in Nd^{3+}-doped calcium aluminosilicate glass, *Appl. Phys. B.*,**77**, 63.
[11]Siegmund, W. P., (**1989**), 'Fiber Optic Tapers in Electronic Imaging', Prepared for Electronic Immaging, West Pasadena, available at Schott Fiber Optics, Southbridge, M.A., USA.

[12] Hurtamnn, P., (**1983**), 'Untersuchungen and glass Szintillation', Ph.D thesis, Universitat. Mainz.
[13] Rakov, N., de Araújo, C., Messaddeq, Y. and Aegeter, M. A., (**1997**), Appl. *Phys. Lett.*, **70**, 3084.
[14] Wade, S. A., Collins, S.F. and Baxter, G. W., (**2003**), *J. Appl. Phys*., **94**, 4743.
[15] Fernández, J., Balda, R., Mendioroz, A. and Adeva, A. J. G., (**2001**), *J. Phys. Condens.Matter*, **13**, 10347.
[16] Chen, G. Y., Zhang, Y. G., Somesfalean, G. and Zhang, Z. G., (**2006**), *Appl. Phys. Lett.*, **89**, 163105.
[17]Tanabe, S., Yoshii, S., Hirao, K. and Soga, N., (**1992**), *Phys. Rev. B*, **45**, 4620.
[18] Tanabe, S., Hirao, K. and Soga, N., (**1990**), *J. Non-Cryst. Solids*, **122**, 79.
[19] Balda, R., Fern´andez, J., Arriandiaga, M.A. and Fdez-Navarro, J. M., (**2004**), *J. Opt.Matter*, **25**, 157.
[20] Gouveia-Neto, A. S., da Costa, E. B., Bueno, L. A. and Ribeiro, S. J. L., (**2004**), *J. Alloys Compd.*, **375**, 224-228.
[21]Tsuboi, T., (2000), *Phys. Rev. B*, **62**, 4200.
[22] Grishin, I. A., Guryev, V. A., Savikin, A. P. and Zvonkow, N. B., (**1995**), *J. Opt. Fiber Technol.*, **1**, 331-336.
[23]Ivanova, T. Y., Manshina, A. A., Kurochkin, A. V., Tveryanovich, Y. S. and Smirnov, V. B., (**2002**), *J. Non-Cryst. Solids*, **298**, 7-11.
[24]Munoz-Matin, D., Villegas, M. A., Gonzalo, J. and Fernandez-Navarro, J. M., (**2009**), *J. Eur. Ceram. Soc.*, **29**, 2903–2913.
[25]Wanga, G., Zhanga, J., Daia, S., Wena, L., Yanga, J. and Jianga, Z., (**2005**), *J. Mol. Struct.*, **750,** 1-6.
[26]Ok, K. M., Bhuvanesh, N. S. P. and Shiv H. P., (**2001**), *J. Inorg. Chem.*, 4**0**, 1978-**1980**.
[27]Pascuta, P. and Culea, E., (**2008**), *Mater. Lett.*, **62**, 4127–4129.
[28] Rajendran, V., Palanivelu, N., Chaudhuri, B. K., Goswami, K., (**2003**), *J. Non-Cryst. Solids*, **320**, 195-209.
[29] Sun, H., Zhang, L., Zhao, S., Zhang, J., Yu, C., He, D., Duan, Z., Hu, L. and Jiang, Z.(**2005**), *J. Solid State Commun*., **133**, 357–361.
[30] Sun, H., Yu, C., Duan, Z., Wen, L., Zhang, J., Hu, L. and Dai, S., (**2006**), *Opt. Mater.*, **28**, 448-452.